Journal of Thermal Analysis and Calorimetry, Vol. 60 (2000) 557–570

NON-ISOTHERMAL MODELLING OF HYDROCARBON ADSORPTION ON A GRANULATED ACTIVE CARBON

E. Fiani[*], *L. Perier-Cambry and G. Thomas*

Ecole Nationale Supérieure des Mines de Saint-Etienne, Centre SPIN, 158 cours Fauriel
F-42023 St-Etienne cedex 2, France

(Received December 7, 1998; in revised form July 15, 1999)

Abstract

The adsorption of *n*-butane on extruded cylindrical activated carbon grains is studied providing two kinds of information: the influence of the temperature and the hydrocarbon partial pressure on the adsorption dynamics (kinetic study) and on the adsorption capacities (thermodynamic study). The thermodynamic aspect could be interpreted by a Langmuir model. From a kinetic point of view, we have experimentally proved that strong temperature variations occur inside the particles during the adsorption. In this paper, a kinetic model including both mass and heat transfer phenomena is proposed. Good agreement is found between the kinetic model predictions and the experimental mass and temperature variations inside the grain during the hydrocarbon adsorption.

Keywords: activated carbon, hydrocarbon adsorption, modelling, non-isothermal kinetics

Introduction

Active carbons are well suitable for adsorption processes as they possess very high surface areas due to a very dense texture of micropores usually considered as slit-shaped pores separating disordered aromatic sheets [1]. They can be elaborated from several raw materials (wood, lignite, coconut shell, fruit peat, bituminous coal...) which can be activated by the steam activation process or by the chemical activation process [2]. According to the kind of material and activation mode, numerous geometrical and chemical properties can be obtained for the final product. Consequently, activated carbon-based materials appear in various industrial applications: water treatment [3, 4], precious metal recovery [5], odour treatment [6], gas storage [7]... This work particularly focuses on the case of the removal of fuel vapours evolved from automative vehicle tanks. Evaporative emission of fuel from motor vehicles (running losses, hot soak losses and diurnal losses) is known to be one of the main sources of urban volatile organic compound (VOC) air pollutants [8]: for instance, in 1985, the estimated VOC lost amount due to vehicles on the French terri-

---

[*] Author for correspondence: e-mail: fiani@emse.fr

1418–2874/2000/ $ 5.00

Akadémiai Kiadó, Budapest
Kluwer Academic Publishers, Dordrecht

tory was comprised between 13.7 and 28 g_{VOC} veh^{-1} day^{-1}, according to the type of vehicle [9]. Such vapours exhibit harmful effects on health. Some of the molecules constituting these vapours such as polycyclic aromatic hydrocarbons (benzopyrene, benzoanthracene...) have been proved to be carcinogenic [10]. Others like alkanes or alkenes are essential intermediates for the formation of photochemical smog and thus contribute to the development of eye or lung irritant agents [11, 12].

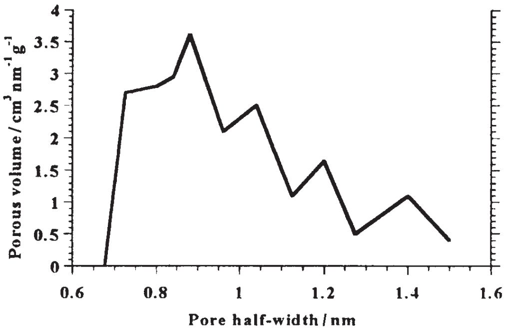

Fig. 1 Pore size distribution from nitrogen adsorption isotherm

The objective of this study consists in following the behaviour of an active carbon in contact with gaseous *n*-butane, a major compound of fuel vapours. Supported by experimental data, a model will be proposed concerning two aspects of *n*-butane adsorption: firstly, a thermodynamic model to predict the active carbon adsorption capacities and, secondly, a kinetic model to describe adsorption dynamics.

Experimental

Activated carbon features and gases

The adsorbent used in this study is composed of cylindrical active carbon grains (5 mm high; 2 mm in diameter) produced by an extrusion process. The density, porosity and porous volume of this granular activated carbon (GAC) are obtained using an AccuPyc 1330 helium pycnometry analyzer (Micromeritics): these ones are respectively 1.60 g cm^{-3}, 0.65 and 1.15 cm^3 g^{-1}. Specific surface area and porous distribution are deduced from the 77 K nitrogen adsorption isotherm obtained from an ASAP 2000 nitrogen porosimetry analyzer (Micromeritics). The isotherm shape is characteristic of microporous materials: it belongs to the type I isotherms according to the international (IUPAC) classification [13]. The conventional BET specific surface area is 1600 m^2 g^{-1}. The active carbon grains exhibit a bimodal porous distribution. From *t*-plots using the Harkins-Jura method, the presence of micropores (half-width less than 1.4 nm) is shown (Fig. 1). These grains also possess very large macropores about 20 μm wide which can easily be seen by Scanning Electron Microscopy (Photograph 1). Such macropores ensure an easy connection of the gaseous phase and the microporous texture; on the other hand, these conclusions are supported by experimental results on the macroporous volume assessment through the mercury intrusion method porosimetry (Fig. 2) using a Porosimeter 2000 (Carlo Erba).

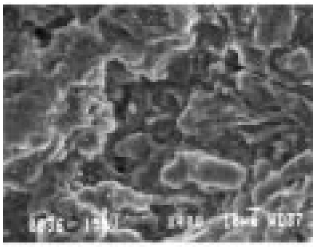

Photograph 1 SEM photograph of the extruded active carbon surface

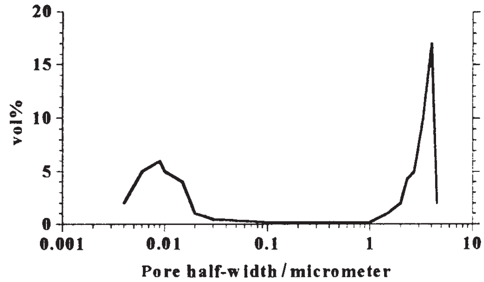

Fig. 2 Pore size distribution from mercury porosimetry

The adsorbent heat capacity C_{p_c} is measured by using a DSC 111 differential scanning calorimeter (Setaram): for temperatures comprised between 20 and 200°C, the C_{p_c} values vary from 0.75 to 1.08 J g^{-1} K^{-1} (Fig. 3).

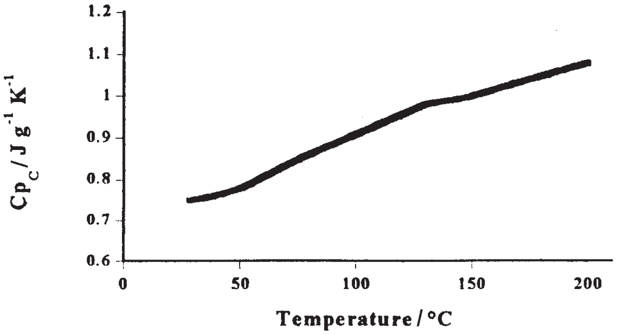

Fig. 3 Variations of the activated carbon heat capacity *vs*. temperature

The pure gases, *n*-butane(purity >99.5% and nitrogen (purity>99.99%), are provided by Air Liquide.

Adsorption of n-butane: experimental procedure

The mass variations of the adsorbent in contact with *n*-butane are measured by thermogravimetric analysis (TG) with a MTB 10-8 thermobalance (Setaram). Figure 5 represents the TGA apparatus.

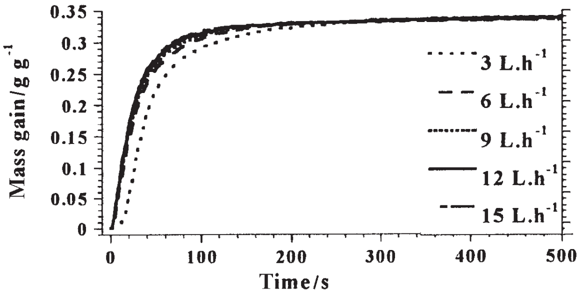

Fig. 4 Influence of the gaseous mixture flow rate upon the kinetic curve shape; p=0.8 atm; T=10°C

The mass of the solid samples is 30 mg. The temperature of the reactor containing the solid sample is set thanks to a thermoregulated water bath. Adsorbed gases are removed from the solid samples before each experiment by a vacuum pump for 2 h. Then the balance is pressurized under one atmosphere of high-purity nitrogen acting as an inert gas towards adsorption on the studied active carbon. We have verified indeed that this gas presents no interaction with the solid surface. Then gaseous *n*-butane is diluted in nitrogen under dynamic conditions at atmospheric pressure and the sample mass gain monitored continuously until equilibrium. Pure nitrogen and *n*-butane are mixed from commercial gas-bottles by using a bank of thermal mass flowmeters (Brooks). After being heated at the same temperature as reactor one, the gaseous mixture is introduced through a small cylindrical tube (2 mm in diameter) just 2 cm under the solid sample (lying on a metal wired square 1×1 cm sample holder). Glass beads fill the dead volume comprised between the gas mixture inlet and the bottom of the reactor. Whenever the gaseous mixture flow rate is too low, this experimental parameter is likely to limit the adsorption rate. This is the reason why the distance between the gas mixture inlet and the sample as well as the gaseous mixture flow rate have been optimized so that no dilution effect occurs. The influence of the gaseous mixture flow upon the kinetic curves shape has been studied for several conditions of *n*-butane partial pressure and temperature. The case of a very fast adsorption is shown on Fig. 4: the lower the temperature and the higher the *n*-butane concentration, the higher should be the influence of the gaseous mixture flow rate. As expected, transient initial effects as well as diffusion phenomena occur for small flow rate values. However, for values greater than 6 l h^{-1}, the kinetic curve shapes do not depend on the mixture flow rate anymore. Each experiment will be therefore carried out with a gaseous mixture flow rate of 12 l h^{-1}.

Strong exothermic effects are expected as the adsorption rate on the studied active carbon as well as the condensation reaction heat exhibit high values. Thus, temperature variations of the inner central part of an extruded grain are also measured during the adsorption thanks to a microthermocouple. A cylindrical hole (0.3 mm in diameter) was made inside an activated carbon grain, along the axis of the cylinder, and the soldered joint of a chromel/alumel thermocouple (0.25 mm wide) was in-

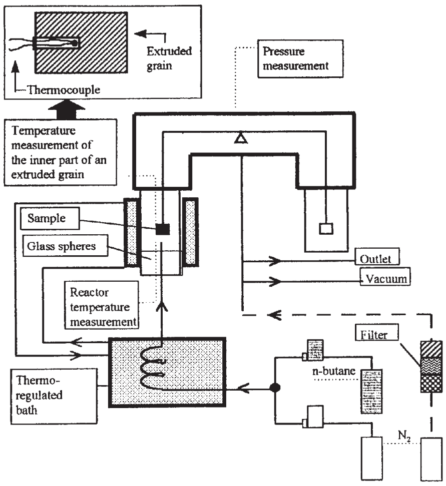

Fig. 5 Schematic diagram of experimental apparatus

serted at the center of the grain and insulated from the outside of the grain. Meanwhile, the reactor temperature is also controlled by a classical thermometer. This original experimental procedure made possible the measurement of temperature variations inside an activated carbon particle due to the energy released by the vapour adsorption.

Adsorption experiments are carried out for seven values of temperature T from –5 to 85°C and for six values of *n*-butane partial pressures p from 0.01 to 0.9 atm.

n-Butane adsorption: thermodynamic aspect

In the literature, numerous thermodynamic models have been proposed to explain the adsorption equilibrium on active carbons: the Langmuir model [14] and its derivatives, the Freundlich model [15], the vacancy solution model (VSM) [16], the Dubinin-Astakhov model [17] and its derivatives [18] or the Toth equation [19] for the most known and used thermodynamic models. One can refer to Khan *et al.* [20] and Parker [21] who have gathered and compared many of these models. Within the temperature and the *n*-butane pressure ranges we have studied, the experimental isotherms can be described by a Langmuirian mechanism (Fig. 6). The adsorbent surface can be regarded as a lattice of active adsorption sites named *s* and characterized by the same binding energy involved when the adsorption occurs. As a consequence, the adsorption can be seen as a chemical equilibrium representing the reaction of s with the gas *G* to yield a new species, G–s, which is the gas fixed on the surface:

$$G+s \leftrightarrow G-s \tag{E1}$$

Let us call K the equilibrium constant for the reaction, P the partial pressure of *n*-butane relative to 1 atmosphere [dimensionless] and θ_e the relative quantity of *n*-butane adsorbed at equilibrium. The mass action law gives:

$$\theta_e = \frac{KP}{1+KP} \tag{1}$$

We will define θ_e (and more generally $\theta(t)$: the fractional amount adsorbed at any time t) as the ratio of the mass m_e of *n*-butane adsorbed at equilibrium per unit mass of adsorbent [$g_{\text{n-butane}}\ g_{\text{GAC}}^{-1}$] (respectively the mass $m(t)$ of *n*-butane adsorbed at any time per unit mass of adsorbent) to m_{tot} [$g_{\text{n-butane}}\ g_{\text{GAC}}^{-1}$] (so called afterwards g g^{-1}):

$$\theta(t) = \frac{m(t)}{m_{\text{tot}}} \tag{2}$$

The symbol m_{tot} refers to the total amount of *n*-butane which can be fixed in the whole porous system corresponding to a unit mass of adsorbent at infinite pressure (sterical limit). The parameter m_{tot} was originally defined by Langmuir as the monolayer capacity. However, since the chemical features of the gaseous molecules are very close to the ones of the chemical groups placed at the activated carbon surface, an adsorbed molecule is likely to become itself a new adsorption site and thus to enable a ‘volume’ adsorption. This general definition of m_{tot} leads to consider ‘true’ surface adsorption and possible volume adsorption the same way. The equation used to fit the experimental thermodynamic data becomes therefore:

$$m_e = m_{\text{tot}}\left(\frac{KP}{1+KP}\right) \tag{3}$$

Furthermore, being an equilibrium constant, K [dimensionless] must follow the Van’t Hoff equation:

$$K = K_o \exp\left(\frac{-\Delta_a H^o}{RT}\right) \tag{4}$$

where

$$K_o = \exp\left(\frac{\Delta_a S^o}{R}\right) \tag{5}$$

where $\Delta_a H^o$ is the standard enthalpy variation for adsorption [J mol^{-1}] and $\Delta_a S^o$ is the standard entropy variation for adsorption [J K^{-1} mol^{-1}].

The assessment of the parameters m_{tot} and $K=f(T)$ is provided by applying the Langmuirian thermodynamic model to the experimental results (Fig. 6). A constant value is obtained for m_{tot} whatever T might be: $m_{\text{tot}}=0.389$ g g^{-1}. The variations of K *vs.* T are reported in Table 1. The influence of T upon K obeys the Van’t Hoff law: the plot of $\ln K=f(1/RT)$ gives effectively a straight line from which $\Delta_a H^o$ and $\Delta_a S^o$ can be deduced $\Delta_a H^o = -22.3$ kJ mol^{-1} and $\Delta_a S^o = -59.4$ J K^{-1} mol^{-1}. The negative values are consistent with the fact that the adsorption phenomenon is exothermic and that *n*-butane changes from a gaseous state to a less disordered condensed matter.

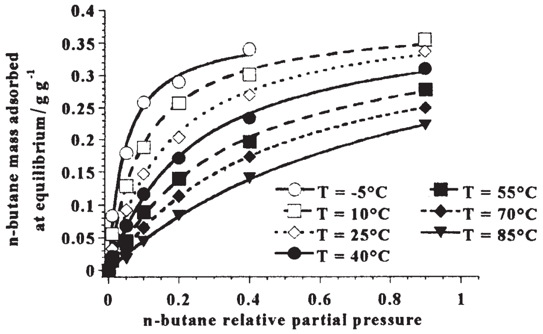

Fig. 6 Isotherms for *n*-butane adsorption compared to Langmuir isotherm predictions

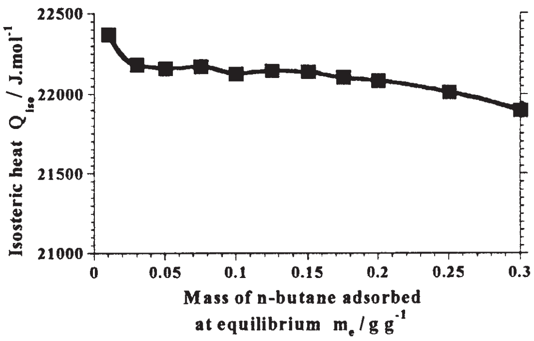

Fig. 7 Variations of the isosteric heat with m_e

Table 1 Langmuirian equilibrium constants for *n*-butane adsorption between 268 and 358 K

T/K	268	283	298	313	328	343	358
K/–	18.6	10.0	5.72	4.05	2.8	2.05	1.41

Moreover, according to the Clausius-Clapeyron equation, adsorption isosteric heat Q_{iso} can be calculated as a function of the mass m_e of *n*-butane adsorbed at equilibrium per unit mass of adsorbent (Fig. 7) from the slopes of $\ln P=f(1/T)$ at fixed values of m_e. Over the whole range of m_e, the isosteric heat of adsorption value is almost constant (22.1 kJ mol^{-1}), which means that each site is characterized by only one binding energy. This observation is in fair agreement with the Langmuir mechanism assumption concerning a homogeneous energetic site distribution. This value is close to $|\Delta_a H^0|$ deduced from the Van't Hoff law. Nevertheless, two shifts are observed on Fig. 7. Firstly, the isosteric heat tends to increase for decreasing values of m_e, from m_e=0.05 g g^{-1}. This means that the first sites involved in the *n*-butane adsorption offer binding energies which are perceptibly stronger than the ones of almost all the sites. Secondly, the isosteric heat seems to decrease for high values of m_e. This is probably due to stronger calculation errors when slopes of the $\ln P=f(1/T)$ curves are estimated for higher values of m_e. As a matter of fact, the points of the $\ln P=f(1/T)$ curve are obtained, for a given value of m_e, from the intersections between the seven experimental isotherms and the horizontal line $y=m_e$ (Fig. 6). So, when m_e is approximatively higher than 0.25 g g^{-1}, it is predictable that the estimation of these intersections are far less accurate since the concerned part of the isotherms is the plateau. One also may consider that for high adsorption pore filling, new endothermic interactions between adsorbed molecules lower the isosteric heat values. At last, it is also remarkable that Q_{iso} and $|\Delta_a H°|$ are very close to the standard enthalpy variation of *n*-butane vaporization which is 21.02 kJ mol^{-1} at 25°C. This is not surprising as non-polar molecule adsorption on non-polar surface is usually considered as a phenomenon of the same nature as condensation from a gaseous state to a liquid-like state.

n-Butane adsorption: kinetic aspect

Results

When the activated carbon surface adsorbs *n*-butane, the experimental apparatus we have conceived enables the simultaneous measurements of the sample mass and the temperature variations inside a granule ΔT_i by a microthermocouple. A typical example of the two coupled data is given on Fig. 8. In most cases, the *n*-butane adsorption is very fast and occurs within a few minutes. The most unfavourable kinetic condition appears at low-temperature and low-pressure (P=0.01 and $T=-5$°C): it takes about 25 min to reach the equilibrium. The usual encountered equilibrium times are comprised between 100 and 300 s. In addition, significant temperature variations have been observed inside the grains during the adsorption though the reactor temperature still remains unchanged. As soon as the first molecules of *n*-butane are fixed, the temperature immediately increases to quickly reach a maximum, then decreases more slowly until $\Delta T_i=0$. Actually, ΔT_i is not exactly nil when the sample mass has become constant. The example given on Fig. 8 shows that it takes 150 s for the mass gain to be constant whereas 200 s are required for ΔT_i to be equal to zero, and ΔT_i =2.5°C at 150 s. These observations are likely to be due to a noticeable accumulation of heat released by the adsorption. The maximum amplitude of ΔT_i is about 1 or 2°C when P=0.01 whatever the temperature might be, and can reach 40°C when P=0.9 and T=10°C.

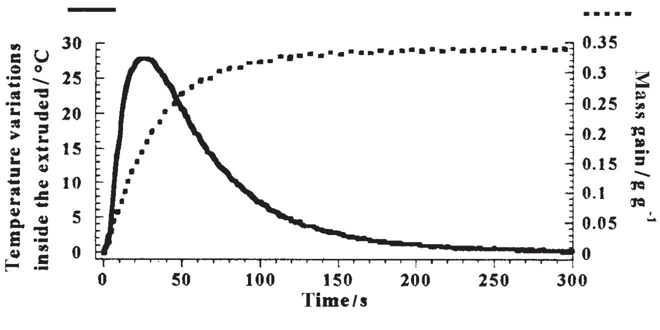

Fig. 8 Example of an uptake curve (---) with thermal effects (–) measured inside an extruded particle; P=0.4; T=268 K

Temperature variations ΔT_s have also been measured at the surface of the grains during the *n*-butane adsorption thanks to another thermocouple fixed at the surface of a grain. It appeared that surface temperature variations ΔT_s are almost equal to the ones of the central part of the granule. Sometimes, surface temperature are slightly lower than the internal ones as it is shown on Fig. 9. This figure represents the case where the difference between ΔT_i and ΔT_s is the widest. Generally, ΔT_i is comprised between $0.7{\cdot}\Delta T_i$ and ΔT_i (in °C). This is probably due to a gentle cooling of the grain surface by the *n*-butane/nitrogen gaseous stream.

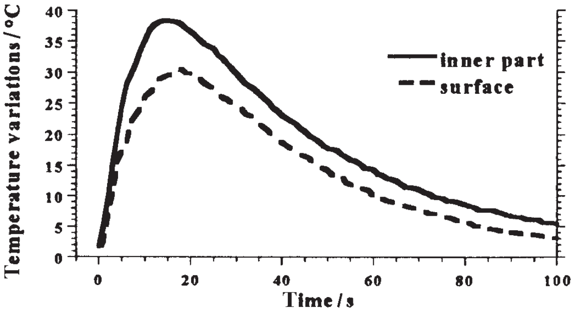

Fig. 9 Comparison of the temperature variations inside (---) and at the surface (–) of a particle during the adsorption; P=0.9; T=283 K

Consequently, the *n*-butane adsorption on the extruded active carbon cannot be considered as an isothermal reaction and the temperature can be considered as uniform inside the particle and equal to the one measured at the centre of the grain.

Discussion

To predict the mass gain and the temperature evolutions of a granular activated carbon sample occurring during *n*-butane adsorption, a kinetic model is required. Several kinetic models concerning adsorption of hydrocarbons on activated carbons have already been proposed in literature [22–25]. However, as far as we know, the existence of strong non-isothermal features has never been reported even in case of granular activated carbons and thus isothermal conditions are assumed in numerous cases. We propose a kinetic model which takes into consideration the non-isothermal feature of our experimental adsorption data. This model results from the expression of the adsorption rate on the one hand, and of the energy balance in the extruded material on the other hand. Therefore, it expresses the interdependence of mass and temperature variations.

Firstly, concerning the adsorption rate calculation, several assumptions about the *n*-butane adsorption mechanisms are proposed, some of them verified from experimental observations (a to c).

a) The number of grains is small enough to avoid any rate limiting step due to diffusion in the gaseous phase, particularly between the particles.

b) The gaseous mixture flow rate has been chosen high enough so that it does not have any effect on the kinetic curve evolution: this way, the adsorption rate cannot be limited by the *n*-butane external diffusion.

c) We have carried out adsorption experiments on cylindrical grains cut from the original ones with a modified height (1 mm high). Then we have compared the results with those obtained from the original grains (5 mm high). Figure 10 shows the kinetic curves of both the original and the smaller grains in the case of two different experimental conditions. As the grain size does not seem to have any effect on the adsorption rate, the access of gases into the microcristallites separated by the very large macropores (Photograph 1) and containing the microporous lattice should be fast: hence it is reasonable to assume that no internal *n*-butane diffusion limitation should happen in the macroporous system.

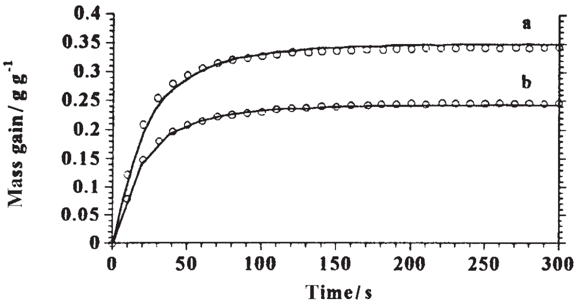

Fig. 10 Comparison between the uptake curves of the original grains (o) and smaller grains (–); a – P=0.9; T=268 K; b – P=0.9; T=343 K

d) After the gas reaches the microcristallite level, the adsorption rate is supposed to be limited by the interfacial reaction rate. We also suppose that this step is governed by a kinetic law deduced from the Langmuir mechanism presented in the thermodynamic section. The equilibrium between the gaseous phase and the adsorbed phase according to the Langmuir mechanism (equilibrium E1) gives the expression of the adsorption rate [s^{-1}] as a function of the relative pressure:

$$\frac{\mathrm{d}\theta(t)}{\mathrm{d}t}=kP[1-\theta(t)]-k'\theta(t) \tag{6}$$

where θ is defined as Eq. (2), k and k' [s^{-1}] are kinetic constants for adsorption and desorption respectively and verify the Arrhenius law at any time t:

$$k=k_\mathrm{o}\exp\left(\frac{-E}{RT_\mathrm{g}(t)}\right) \qquad k'=k'_\mathrm{o}\exp\left(\frac{-E'}{RT_\mathrm{g}(t)}\right) \qquad \text{(7) and (8)}$$

where E and E' are respectively activation energies for adsorption and desorption [J mol^{-1} K^{-1}] and T_g is the grain temperature [K].

E, E', k_o and k'_o are unknown parameters to be calculated. However, these parameters are not independent since they are respectively linked to $\Delta_a H^o$ and K_o determined from the Langmuirian thermodynamic modelling:

$$\Delta_a H^o = E - E' \quad \text{and} \quad K_o = \frac{k_o}{k'_o} \qquad \text{(9) and (10)}$$

The kinetic and thermodynamic aspects are therefore two parts of a global modelling since the expression of the adsorption rate is directly connected to the model describing the variations of hydrocarbon amounts adsorbed at equilibrium with temperature and n-butane partial pressure.

Secondly, as the temperature T_g inside the grains depends on time, the heat balance must be established in the extruded material. For that purpose, as in the first part of the modelling, some assumptions have been put forward.

a) By comparing ΔT_i and ΔT_s occurring with the n-butane adsorption, it is assumed that the temperature inside the particle is uniform and equal to the one measured in the centre of the grain.

b) The heat exchange is mainly insured by forced convection through S [m^2], the external surface area of the adsorbent grains, disregarding the possible roughness of the solid: for one activated carbon grain, S=37.7 mm^2.

c) The heat-transfer coefficient h [W m^{-2} K^{-1}] is calculated in the case of forced convection around grains considered as long cylinders the axes of which are perpendicular to the approaching gas mixture stream. The heat-transfer coefficient is deduced from the Nusselt number predicted from the following dependence of the dimensionless Chilton-Colburn j_H factor with the dimensionless Reynolds, Prandtl and Nusselt numbers (respectively Re, Pr and Nu):

$$j_H = Nu Re^{-1} Pr^{-1/3} \tag{11}$$

as reported by Bird *et al.* [26].

The energy balance within the grain at any given time enables to express the heat produced by n-butane adsorption as the sum of the energy lost by convection at the fluid-solid interface and the energy accumulated inside the grain.

$$\frac{\mathrm{d}m(t)}{\mathrm{d}t}\frac{\Delta_a H^o}{M} - hS(T_g(t) - T) = (m_C C_{p_C} + m(t) C_p)\frac{\mathrm{d}T_g(t)}{\mathrm{d}t} \tag{12}$$

where M is the n-butane molecular mass [g mol^{-1}], C_p and C_{p_C} are respectively the heat capacities of n-butane and of the active carbon [J mol^{-1} K^{-1}] and m_C is the mass of an extruded activated carbon grain [g].

The equation system composed of the two dependent Eqs (6) and (12) allows to calculate the grain temperature T_g and mass m variations with time. A Turbo-Pascal code has been developed to calculate T_g and m step by step by time increments, with the initial conditions $T_{g(t=0)}=T$ and $m_{(t=0)}=0$. As seen previously, four characteristic parameters are unknown and must be derived: E, E', k_o and k'_o.

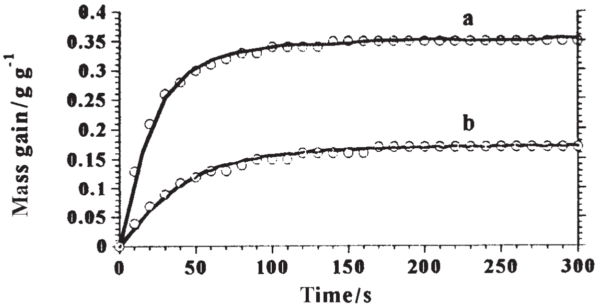

Fig. 11 Mass gain *vs.* time: experiment (–) and model (o) for two examples: a – T=10°C and P=0.9; b – T=40°C and P=0.2

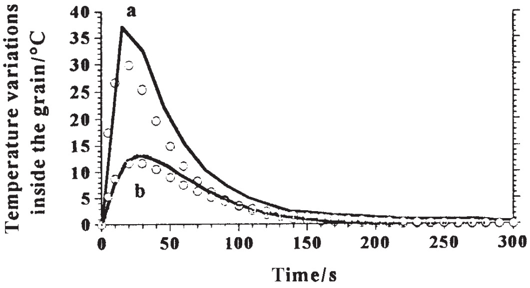

Fig. 12 Internal temperature variation *vs.* time: experiment (–) and model (o) for two examples: a – T=10°C and P=0.9; b – T=40°C and P=0.2

Since K_o and $\Delta_a H^\circ$ are calculated from the thermodynamic modelling, only two parameters have to be estimated. They should be determined so that, being constant, they allow the model equation system to correctly describe each adsorption kinetic curve. If k'_o=1010 s^{-1} (i.e. k_o=0.800 s^{-1}), the fitted values of E' are nearly constant and little dispersed around an average of 29.5 kJ mol^{-1} K^{-1} (i.e. E=7.2 kJ mol^{-1} K^{-1}) for the non-isothermal Langmuirian kinetic model to present a fairly good agreement with the 41 experimental kinetic curves. Figures 11 and 12 compare the experimental and predicted curves respectively for the activated carbon mass gain and for the internal temperature

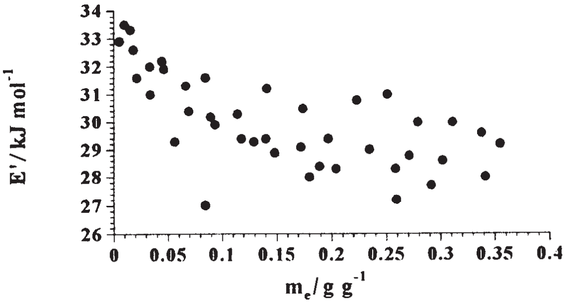

Fig. 13 Variations of the fitted values of E' *vs.* m_e

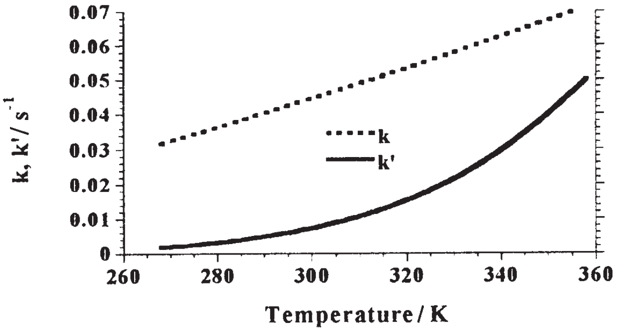

Fig. 14 Variations of k and k' *vs*. temperature when E=7.2 kJ mol^{-1}, E'=29.5 kJ mol^{-1}, k_o=0.800 s^{-1}, k'_o=1010 s^{-1}

variations in the case of two very different P–T conditions. Small variations of the fitted values of E' around 29.5 kJ mol^{-1} seem to be caused by the slight heterogeneity supposed to be on the adsorbent surface when m_e<0.05 g g^{-1}: values of E' *vs.* m_e are plotted on Fig. 13 and vary the same way as isosteric heat ones do (Fig. 7). Kinetic curves for the adsorption of *n*-butane on a granulated active carbon can therefore be predicted from the combination of the expression of the adsorption rate assuming a Langmuir mechanism and of the grain heat balance. The calculated energy of activation E is very low and the variations of k and k' with temperature according to Eqs (4) and (5) are reported on Fig. 14. Non-polar organic vapours are usually considered as physical by Van der Waals forces and in particular London dispersion attractive forces [27]. Besides the fast rates of *n*-butane adsorption experimentally observed and the adsorption enthalpies close to the gas condensation enthalpy, this poor value for E is consistent with a physical adsorption involving low activation energies.

Conclusions

The adsorption of *n*-butane was studied on a granular activated carbon showing a bimodal porous distribution and a fairly homogeneous site distribution, for a wide range of temperature and *n*-butane partial pressure conditions. Experimental data were obtained by using a thermogravimetric apparatus adapted to enable the measurements of the temperature of the inner part of the extruded particles during the adsorption. Strong temperature variations can be observed this way. The thermodynamic aspect of the adsorption can be well explained by the Langmuir equation. On the kinetic side, a model constituted of two parts has been developed to predict both adsorbent mass and temperature variations during the adsorption. Firstly, the adsorption rate is expressed assuming an interfacial limiting step corresponding to a Langmuir mechanism. Secondly, the heat balance is written inside the adsorbent grains assuming a fast conduction in the grains. Good agreement is found between experimental mass and temperature variations and the predictions of our kinetic model taking into account the interdependence of both variations. The slight heterogeneity of the activated carbon seems to cause little variations of E' with m_e and the low value found for E is consistent with a poorly activated adsorption.

References

1 H. F. Stoeckli, Carbon, 28 (1990) 1.
2 A. Ahmadpour and D. D. Do, Carbon, 34 (1996) 471.
3 D. W. Hand, J. C. Crittenden and W. E. Tacker, J. Environ. Eng., 109 (1883) 82.
4 J. T. Paprowicz, Env. Tech., 11 (1990) 71.
5 M. Zarrouki, Analusis, 18 (1990) 261.
6 G. Martin, M. Lemasle and S. Taha, Poll. Atm., 136 (1993) 128.
7 S. Sircar, T. C. Golden and M. B. Rao, Carbon, 34 (1996) 1.
8 A. B. Hansen and F. Palmgren, Sc. Tot. Env., 189 (1996) 451.
9 R. Bouscaren and N. Allemand, Poll. Atm., 123 (1989) 273.
10 M. Chiron, P. Quénel and D. Zmirou, Poll. Atm., 153 (1997) 41.
11 R. A. Cox, Poll. Atm., special issue (July 1991) 9.
12 R. Bouscaren, Poll. Atm., 123 (1989) 269.
13 G. L. Aranovich and M. D. Donohue, Carbon, 33 (1995) 1369.
14 I. Langmuir, J. Chem. Soc., 40 (1918) 1361.
15 H. Freundlich, Colloid and Capillary Chemistry, Mathuen, London 1926, p. 110.
16 T. W. Cochran, R. L. Kabel and R. P. Danner, AIChE, 31 (1985) 2075.
17 R. C. Bansal, J. B. Donnet and F. Stoeckli, Active Carbon, Dekker, New York 1988.
18 N. Sundaram, Langmuir, 9 (1993) 1568.
19 J. Toth, Acad. Sci. Hung., 69 (1971) 311.
20 A. R. Khan, R. Ataullah and A. Al-Haddad, J. Colloid Interface Sci., 194 (1997) 154.
21 G. R. Parker, Adsorption, 1 (1995) 113.
22 T. F. Lin, J. C. Little and W. W. Nazaroff, J. Env. Eng., 122 (1996) 169.
23 M. L. Zhou, PhD thesis, Rennes, 1992.
24 P. L. J. Mayfield and D. D. Do, Ind. Eng. Chem. Res., 30 (1991) 1262.
25 J. Fettig and H. Sontheimer, J. Env. Eng., 113 (1987) 764.
26 R. B. Bird, W. E. Steward and E. N. Lightfoot, Transport phenomena, Wiley, New York 1960.
27 R. H. Bradley and B. Rand, J. Colloid Interface Sci., 169 (1995) 168.